

MOL 39008

Lipid composition alters drug action at the nicotinic acetylcholine receptor

**John E. Baenziger*, Stephen E. Ryan, Michael M. Goodreid, Ngoc Q. Vuong, Raymond M.
Sturgeon, and Corrie J.B. daCosta**

**From the Department of Biochemistry, Microbiology, and Immunology, University of
Ottawa, Ottawa, Ontario, Canada K1H 8M5**

MOL 39008

Running title: Bilayer lipid composition influences drug action at the nAChR

Corresponding author:

John Baenziger, Department of Biochemistry, Microbiology, and Immunology, University of
Ottawa, 451 Smyth Rd., Ottawa, ON, Canada, K1H 8M5. Tel.: (613) 562-5800x8222; Fax: (613)
562-5440, Email: jebaenz@uottawa.ca.

Number of text pages: **32**

Number of tables: **2**

Number of figures: **7**

Number of references: **40**

Number of words in Abstract: **238**

Number of words in Introduction: **736**

Number of words in Discussion: **1404**

¹The abbreviations used are: nAChR, nicotinic acetylcholine receptor; Carb, carbamylcholine,
TMA, tetramethylamine; PC, phosphatidylcholine; PA, phosphatidic acid; Chol, cholesterol,
FTIR, Fourier transform infrared; ATR, attenuated total reflectance.

MOL 39008

Abstract

We tested the hypothesis that membrane lipid composition influences drug action at membrane proteins by studying local anesthetic action at the nicotinic acetylcholine receptor (nAChR). Infrared difference spectra show that concentrations of tetracaine consistent with binding to the ion channel ($<50\ \mu\text{M}$) stabilize a resting-like state when the nAChR is reconstituted into phosphatidylcholine membranes containing the anionic lipid, phosphatidic acid, but have no effect on the nAChR reconstituted into membranes lacking phosphatidic acid, either in the presence or absence of cholesterol. Concentrations of tetracaine above $200\ \mu\text{M}$ lead to neurotransmitter site binding in all membranes. In the presence of phosphatidic acid and/or cholesterol, neurotransmitter site binding leads to the formation of quaternary amine-aromatic interactions between tetracaine and binding site tyrosine/tryptophan residues and the stabilization of a desensitized state. One interpretation suggested by lipid partitioning studies is that phosphatidic acid enhances tetracaine action at the channel pore by increasing the partitioning of tetracaine into the lipid bilayer and thus enhancing access to the transmembrane pore. Subtle membrane-dependent variations in the vibrations of tyrosine and tryptophan residues, as well as agonist analog binding studies, however, indicate that the structures of the agonist-bound neurotransmitter sites of the nAChR in membranes lacking both phosphatidic acid and cholesterol differ from the structures of the agonist-desensitized neurotransmitter sites in the presence of both lipids. Lipid action at the nAChR thus involves more than a simple modulation of the equilibrium between resting and desensitized states.

MOL 39008

Introduction

Many of the complex and diverse functions of biological membranes are intimately dependent upon the interactions that occur between lipids and proteins. Numerous integral membrane proteins, including the nicotinic acetylcholine receptor, are dependent upon lipid bilayer composition for optimal activity (Lee, 2004; Barrantes, 2002, 2004). Membrane protein function can be regulated by the association of proteins with lipid microdomains/rafts (Allen et al., 2007; Szabo et al., 2007). Conversely, numerous proteins can influence the physical properties and/or the two-dimensional packing of lipids in a biological membrane (McMahon and Gallop, 2005; daCosta et al., 2002).

Given the intimate relationship between both lipid and membrane protein structure and function, it seems likely that lipid bilayers influence drug action at membrane protein targets. It has been suggested that drug induced perturbations in bulk membrane physical properties/fluidity may alter membrane protein function, although in many cases protein binding sites for lipophilic drugs have been identified (Miller, 2002). Alternatively, drugs could indirectly influence membrane protein activity by disrupting the formation of and/or association of proteins with lipid rafts (Szabo et al., 2007). Changes in lipid composition, as a protein target shuttles in and out of a raft, or as a consequence of diet, etc., could also influence drug action by stabilizing the target protein in conformations that bind drugs with different affinities. Given that over 50% of all drug targets are membrane proteins, understanding how drug action is influenced by the lipid bilayer is clearly of importance (Overington et al., 2006).

In this report, we use Fourier transform infrared (FTIR¹) difference spectroscopy to examine how lipid environment influences the ability of a local anesthetic to modulate the conformational equilibria of the nicotinic acetylcholine receptor (nAChR¹) from the electric fish

MOL 39008

Torpedo. The nAChR is the prototype of the Cys-loop family of neurotransmitter-gated ion channels, whose members are found at synapses throughout the peripheral and central nervous systems (Sine and Engel, 2006; Lester et al., 2004). The nAChR is an excellent model for testing how lipids influence drug action because it has been used extensively for independently studying both lipid-protein and drug-receptor interactions (Arias et al., 2006; Ryan et al., 1996; Baenziger et al., 2000; Fong and McNamee, 1986).

We first examine the conformational effects of the local anesthetic, procaine, at the nAChR to test the utility of the spectroscopic technique for monitoring local anesthetic induced conformational change. We chose to study this local anesthetic because its effects on nAChR conformational state are unclear (Krodel et al., 1979). Most local anesthetics bind to mutually exclusive non-competitive inhibitor sites in the channel pore and are thought to stabilize the nAChR in a desensitized conformation. Procaine, unlike most local anesthetics, binds with higher affinity to the neurotransmitter sites ($K_D = 930 \mu\text{M}$) than to its allosteric non-competitive inhibitor site in the ion channel ($K_D = 3000 \mu\text{M}$) (Blanchard et al., 1979). As procaine competes directly with acetylcholine for binding, acetylcholine binding assays have not detected a procaine-induced change in acetylcholine binding affinity associated with the stabilization of either a resting or desensitized state. Our goal here was to test whether FTIR difference spectroscopy, which monitors directly ligand-induced nAChR structural change, can detect a procaine-induced conformational shift that has not been detected using classical ligand-binding experiments.

We next examine the conformational effects of the local anesthetic, tetracaine, on the nAChR reconstituted into membranes composed of phosphatidylcholine (PC) either with or without phosphatidic acid (PA) and/or Cholesterol (Chol). The specific membrane environments

MOL 39008

were chosen because of their varying abilities to stabilize the nAChR in a functional state (Baenziger et al., 2000). The local anesthetic, tetracaine, was chosen because it has complex effects at the nAChR. Tetracaine binds to its allosteric non-competitive inhibitor site in the channel pore ($K_D = 1.5 \mu\text{M}$) where it stabilizes the nAChR in a low affinity agonist binding and thus putative resting conformation (Blanchard et al., 1979, Boyd and Cohen, 1980). Tetracaine also binds at higher concentrations ($K_D = 800 \mu\text{M}$) to the neurotransmitter sites and stabilizes a desensitized state (Blanchard et al., 1979, Ryan and Baenziger, 1999).

Our results show that the ability of tetracaine to modulate nAChR conformational equilibria is dependent upon lipid environment. Drug action at the nAChR and possibly other neurotransmitter receptors is sensitive to membrane lipid composition. Our data demonstrate the utility of FTIR difference spectroscopy for monitoring drug action at membrane protein targets and provide insight into the mechanisms by which lipids alter drug action at the nAChR.

MOL 39008

Materials and Methods

Materials. Electric tissue from *Torpedo californica* was purchased from Aquatic Research Consultants (San Pedro, CA). Tetracaine, procaine, carbamylcholine (Carb), and cholesterol (Chol) were from Sigma-Aldrich (St. Louis, MO). Egg phosphatidylcholine (referred to as PC) and dioleoylphosphatidic acid (referred to as PA) were from Avanti polar lipids (Alabaster, Al).

Sample Preparation. The nAChR was affinity purified and reconstituted into membranes composed of either PC, PC/Chol 3:2 (mol/mol), PC/PA 3:2 (mol/mol), and PC/PA/Chol 3:1:1 (mol/mol/mol) as described in detail elsewhere (daCosta et al., 2002). The affinity purifications were performed using a derivatized Affi-Gel 102 (Bio-Rad, Hercules, CA) column prepared as follows. 10-15 mls of Affi-Gel 102 was incubated with 3.5 g of N-acetyl-DL-homocysteinethiolactone overnight at pH 9.7 to generate a sulfhydryl reactive group. The following morning, the gel was washed extensively with 0.1 M NaCl and incubated with 25 mls of 0.08 M dithiothreitol (Sigma, St. Louis, MO) in 200 mM Tris, pH 8. After 30 minutes, the gel was washed with 100mM NaCl in 20 mM Na₂HPO₄ to remove all dithiothreitol and the activated resin reacted with 0.4 g of bromoacetylcholine bromide in 15 mls of 50 mM Na₂HPO₄, pH 7 for one hour. The gel was then washed with several column volumes of 200 mM Tris, pH 8 and incubated with 0.1 g of iodoacetamide to block remaining free sulfhydryl groups.

Aliquots for analysis by FTIR were prepared by depositing 250 µg of nAChR protein in the chosen lipid environment on the surface of a germanium internal reflection element (see Fig. 1, supplemental information). In each case, the excess buffer was evaporated with a gentle stream of N₂ gas and the nAChR film rehydrated with excess *Torpedo* Ringer buffer (250 mM

MOL 39008

NaCl, 5 mM KCl, 2 mM MgCl₂, 3 mM CaCl₂, and 20 mM Tris, pH 7.0). Each sample was placed in a thermostatically controlled attenuated total reflection cell (Harrick Scientific; Ossining, New York).

FTIR Spectroscopy. All infrared spectra were acquired using the attenuated total reflectance (ATR) technique on either an FTS-40 or an FTS-575 spectrometer equipped with a DTGS detector. Spectra were recorded at 8 cm⁻¹ resolution using 512 scans each, which took roughly 7 minutes per spectrum. Consecutive spectra of the resting nAChR were recorded while flowing *Torpedo* Ringer buffer past the nAChR film surface. The flowing solution was then switched to an identical buffer containing 50 μM Carb and a spectrum recorded of the desensitized state. The difference between the two resting state spectra (control spectra) and the consecutive resting and desensitized state spectra (referred to as a Carb difference spectrum) were calculated, stored, and the flowing solution switched back to buffer without Carb. After a 20 minute washing period to remove Carb from the film, the process was repeated many times.

The effects of procaine and tetracaine on the structure of the nAChR were probed by recording Carb difference spectra as described above while maintaining the nAChR in the continuous presence of the local anesthetic (the local anesthetic was included in both the plus and minus Carb buffers). For each tetracaine concentration, Carb difference spectra were recorded from a minimum of two different nAChR films. Each presented difference spectrum is the average of more than 40 individual difference spectra. Spectra were interpolated to a resolution of 4 cm⁻¹ and were baseline corrected between 1760 and 1500 cm⁻¹.

Dose response curves. Dose response curves were calculated by measuring band intensities in each spectrum relative to the same band intensities observed in the absence and presence of “saturating” concentrations of local anesthetic. For each band, its intensity in a

MOL 39008

given spectrum was measured relative to an adjacent baseline point. For example, the band intensities at both 1545 and 1515 cm^{-1} were measured in each spectrum relative to the baseline at 1527 cm^{-1} . Data are plotted as the percent change in intensity. The positive bands at 1655, 1545, and 1515 cm^{-1} , and the negative band near 1620 cm^{-1} decrease in intensity in the presence of the local anesthetic, so the 100% value refers to the intensity of the band in spectra recorded in the absence of local anesthetic and the 0% value refers to the intensity of the same band in spectra recorded at the highest local anesthetic concentration. The positive band at 1663 and the negative bands at 1605, and 1273 cm^{-1} first appear and then increase in intensity with the addition of local anesthetic, so the 100% and 0% values correspond to the intensities in spectra recorded at the highest concentration of local anesthetic and in the absence of local anesthetic, respectively. Data were analyzed using a sigmoidal dose-response curve in Graph Pad Prism version 4 (see Table 1S of supplemental information). Except where noted, each EC_{50} value presented in Table 1 is the average of two EC_{50} values obtained by monitoring the intensity changes of two separate infrared difference bands – 1655 and 1545 cm^{-1} for the peptide backbone conformational change to the desensitized state, 1605 and 1273 cm^{-1} for the binding (and subsequent displacement upon Carb binding) of local anesthetic to the neurotransmitter site, and 1620 and 1515 cm^{-1} for the formation of physical interactions between local anesthetic and aromatic binding site residues (see text).

Note that each spectrum used to generate a difference band intensity at a given local anesthetic concentration is the average of between 30 and 60 individual difference spectra and thus 30 to 60 separate experiments. This large number of experiments is necessary to obtain spectra with sufficient signal-to-noise ratio and takes at least two days of spectrometer time. Consequently, it is not feasible to obtain spectra at the number of local anesthetic concentrations

MOL 39008

required to precisely define the dose-response relationships. Does response curves were calculated to assess which spectral features appear or disappear at local anesthetic concentrations consistent with tetracaine binding to its non-competitive inhibitor versus the neurotransmitter binding sites. Statistics for the individual curve fits are presented in Table 1S of the supplemental information.

Tetracaine Partitioning into lipid bilayers. The partition coefficient of tetracaine into each membrane environment was determined as described by Romsicki and Sharom, 1999. Briefly, duplicate membranes at a lipid concentration of 10 mg/ml were equilibrated with 100 μ M tetracaine at 22 °C for 24 hours under constant gentle stirring. The samples were then pelleted at 36000g for 40 min at 22 °C. The tetracaine remaining in the supernatant was determined by measuring the absorbance at 310 nm. Partition coefficients were defined as described in Table 2.

MOL 39008

Results

Fourier transform Infrared (FTIR) spectroscopy as a tool for monitoring local anesthetic-induced conformational change. Infrared spectroscopy probes the frequencies of molecular vibrations, which are sensitive to the chemistry and local environments surrounding functional groups located within a protein. Although the technique is inherently sensitive to local protein structure, it is not commonly used for detailed mechanistic studies of receptor-drug interactions. This is because each residue in a protein gives rise to multiple infrared active vibrations. Protein infrared spectra therefore contain thousands of overlapping bands. The extensive band overlap leads to broad, featureless spectra, from which it is difficult to access residue-specific vibrational, and thus structural, information.

Under careful data acquisition conditions, however, the difference between spectra recorded from a protein stabilized in two different conformational states will reveal bands from only those residues whose molecular vibrations, and thus local structures, change during the conformational transition (Vogel and Siebert, 2003, Kötting and Gerwert, 2005). Difference spectroscopy provides detailed insight into the nature of protein conformational change at the single residue level. For example, the technique has detected changes in the protonation state and/or hydrogen bonding of individual residues during the light activated photocycles of bacteriorhodopsin and the photoactive yellow protein, etc. (Brudler et al., 2001, Kötting and Gerwert, 2005). The detected changes in hydrogen bonding, etc., are often observed at a resolution not achievable with techniques, such as X-ray crystallography.

The difference between infrared spectra of the nAChR recorded in the presence and absence of the agonist, carbamylcholine, (a “Carb difference spectrum”), exhibits a number of overlapping positive and negative bands (Figs. 1-6). These bands are absent in the difference

MOL 39008

between two spectra of the nAChR recorded both in the absence of ligand (data not shown, but see Hill and Baenziger, 2006). They are also absent in control Carb difference spectra recorded from nAChR membranes that have been pre-treated with the competitive antagonist, α -bungarotoxin (Baenziger et al., 1993). These control studies show that the detected vibrational difference bands arise specifically from the structural changes induced in the nAChR upon Carb binding. Only those receptors that are accessible to Carb are thus probed in this assay. Parallel functional studies show that the nAChR in similar films undergoes Carb-induced desensitization (Baenziger et al., 1992). Positive and negative difference bands thus provide a vibrational map of the structural changes that occur in the nAChR upon Carb binding and the resting to desensitized conformational change.

Of particular interest are difference bands in the amide I (1640 to 1670 cm^{-1}) and amide II (1520 to 1580 cm^{-1}) regions (Fig. 1B, trace i). These bands arise from the vibrations of functional groups located in the polypeptide backbone (Jackson and Mantsch, 1995). Positive amide I bands, due primarily to peptide C=O stretching vibrations coupled to C-N stretching, are observed near 1663 cm^{-1} and 1655 cm^{-1} . Positive amide II bands, due to coupled peptide N-H bending and C-N stretching vibrations, are observed centered near 1545 cm^{-1} (Jackson and Mantsch, 1995). Previous studies have shown that these difference bands reflect a change in both the orientation and hydrogen bonding of a region (or regions) of the polypeptide backbone that is (or are) highly accessible to aqueous solvent (Baenziger and Chew, 1997; Hill and Baenziger, 2006). Given both the relatively large changes in structure that occur upon ligand binding to the binding site “C-loop” and the relative solvent accessibility of this region of the polypeptide backbone, it was suggested previously that the vibrational changes that result from the closing of the C-loop around Carb upon transition from the unliganded resting to the liganded

MOL 39008

desensitized state may dominate the spectral features observed in the amide I and II regions of the Carb difference spectrum (Hill and Baenziger, 2006). Regardless, these noted bands serve as markers of the ability of the nAChR to undergo the resting to desensitized conformational transition (Ryan et al., 1996).

Four protein side chain vibrations centered near 1690, 1668, 1620, and 1515 cm^{-1} are also of interest, as they reflect vibrational shifts that result from the formation of physical interactions between Carb and neurotransmitter binding site residues. Positive and negative bands near 1690 and 1668 cm^{-1} , respectively, reflect a shift in the vibrational frequency from 1668 cm^{-1} to 1690 cm^{-1} of an as yet unassigned residue upon formation of a physical interaction (likely a hydrogen bond) with the ester carbonyl functional group of Carb (Ryan et al., 2002). Note that the negative 1668 cm^{-1} vibration is masked by the above discussed positive amide I difference band near 1663 cm^{-1} (Fig. 1B, trace i). Consequently, the vibrations of both bands are not observed as distinct peaks in Carb difference spectra recorded in the absence of local anesthetics. At high concentrations of local anesthetic, however, the intensity near 1663 cm^{-1} disappears providing an unobstructed view of the 1668 cm^{-1} vibration (see below and, for example, trace iii in Fig. 1B).

The negative and positive bands centered near 1620 cm^{-1} and 1515 cm^{-1} , respectively, are characteristic of tryptophan and tyrosine side chains, respectively (Barth, 2000). A previous study suggested that these vibrational bands appear upon binding and the formation of physical interactions between Carb and aromatic residues (Ryan and Baenziger, 1999). As several aromatic residues are located in the binding site (Unwin, 2005; Zhong et al., 1998), the changes in band intensity at these two frequencies may result from the formation of cation- π electron interactions between Carb and binding site tryptophan and tyrosine residues. Here, we use these four vibrations to assess both the nature of Carb-nAChR interactions in each membrane

MOL 39008

environment and how local anesthetic binding to the neurotransmitter sites influences Carb–nAChR physical interactions.

Finally, bands in the difference spectrum near 1724 and 1473 cm^{-1} have been assigned to the vibrations of nAChR-bound Carb (Baenziger et al., 1993). The absolute intensities of these vibrations are essentially constant in difference spectra recorded from sample to sample when spectra are recorded at saturating concentrations of Carb. This is because the multilamellar nAChR films extend well beyond the penetration depth of the evanescent wave of the infrared radiation (see supplemental Figure 1S).

Conformational effects of procaine on the nAChR in PC/PA/Chol 3:1:1. To demonstrate the utility of FTIR spectroscopy for monitoring local anesthetic-nAChR interactions, we recorded Carb difference spectra while maintaining the nAChR in the continuous presence of the local anesthetic, procaine (see supplemental Fig. 1S for a schematic diagram of the data acquisition protocol). Carb difference spectra recorded in the presence of increasing concentrations of procaine are presented as a stacked plot in Figure 1A. This presentation shows clearly that positive difference bands centered near 1724, 1690, and 1473 cm^{-1} are essentially unaffected by the presence of procaine, while relatively large dose-dependent intensity changes are observed at frequencies near 1668, 1655, 1620, 1605, 1545, and 1515 cm^{-1} . The nature of the dose dependent changes can be seen more clearly in the representative difference spectra recorded at 0, 100 μM , and 6 mM procaine (Fig. 1B). The dose dependences of the spectral changes are plotted in Figure 1C with the corresponding values of EC_{50} listed in Table 1.

The procaine-induced changes in the intensities of the amide I and II “marker” bands suggest that procaine does induce a conformational shift in nAChR equilibrium. Specifically, there are dose dependent decrease in intensity centered near 1655 and 1663 cm^{-1} leading to the

MOL 39008

appearance of the underlying negative band centered near 1668 cm^{-1} (this is the negative couple of the 1690 cm^{-1} difference band noted above). The loss of amide I intensity is coupled to a decrease in amide II band intensity centered near 1545 cm^{-1} . These spectral changes are essentially identical to those that have been observed in Carb difference spectra recorded in the presence of the desensitizing local anesthetic, dibucaine (Ryan and Baenziger, 1999). The loss of intensity indicates that the nAChR does not undergo a Carb-induced transition from the resting to the desensitized state in the presence of procaine, likely because procaine already stabilizes a desensitized nAChR.

Note that the spectral changes suggestive of desensitization occur concomitant with the appearance of new negative bands at frequencies that match the vibrations of procaine itself (one of these at 1605 cm^{-1} is designated with a dashed line in Fig. 1B). The negative procaine vibrations appear because procaine bound to the neurotransmitter sites is displaced upon Carb binding (see lower schematic in supplemental Fig. 1S B). The increased negative intensity with increasing procaine concentration reflects increased binding of procaine to the neurotransmitter sites and provides a means of assessing the affinity of procaine for the neurotransmitter sites (Fig. 1C).

The spectral changes indicative of procaine binding also occur concomitant with a reduction in the intensities of both the negative and positive bands near 1620 cm^{-1} and 1515 cm^{-1} , although the latter shifts up in frequency to 1516 cm^{-1} in the presence of procaine. As noted, these two bands are characteristic of tryptophan and tyrosine residues, respectively (Barth, 2000), and likely reflect the formation of cation- π electron interactions between Carb and binding site aromatic residues. Procaine binding to the neurotransmitter sites may reduce the intensities near 1620 and 1515 cm^{-1} in Carb difference spectra by forming similar, but weaker,

MOL 39008

cation- π electron interactions with the same binding site tyrosine and tryptophan residues prior to Carb binding.

Note that at high concentrations of procaine, the loss of the positive amide I bands near 1663 and 1655 cm^{-1} reveals the underlying intensity of the negative protein side chain vibration near 1668 cm^{-1} , which is coupled to the positive side chain vibration near 1690 cm^{-1} . The intensities and frequencies of these two bands are essentially identical to those of the two bands in Carb minus tetramethylamine difference spectra (Ryan et al., 2000), where the vibrations of the two bands can also be seen clearly due to the absence of overlapping amide I vibrations. As noted, the 1690 and 1668 cm^{-1} bands reflect a vibrational shift in an as yet unidentified residue that interacts directly with the ester carbonyl of Carb (Ryan et al., 2000). The fact that procaine binding to the neurotransmitter site has no effect on the frequencies or intensities of these two bands shows that although procaine interacts with aromatic residues in the neurotransmitter sites, it does not form a hydrogen bond with the residue that typically interacts with the ester carbonyl of Carb. The presence of an aromatic moiety on procaine adjacent to the ester carbonyl (Fig. 1C of supplemental information) must sterically prevent procaine from binding effectively to the “esterophilic” subsite in the neurotransmitter binding site.

The different vibrational changes indicative of procaine binding to the neurotransmitter sites appear with an EC_{50} of 590 μM , which is essentially equivalent to the EC_{50} for the procaine-induced changes in nAChR conformational state (540 μM ; Table 1) and similar to the reported affinity of procaine for the neurotransmitter binding sites ($K_D = 930 \mu\text{M}$) (Blanchard et al., 1979). The FTIR data show that procaine binds to the neurotransmitter sites, weakly mimics the quaternary amine-aromatic physical interactions that normally occur between Carb and neurotransmitter binding site tyrosine and tryptophan residues - but not the Carb ester-nAChR

MOL 39008

physical interactions. The data also suggest that procaine stabilizes the nAChR in a desensitized state.

By directly monitoring the structural changes that occur in the nAChR, FTIR detects a procaine induced conformational change that is not detected using traditional ligand binding approaches (Krodel et al., 1979). FTIR provides a means of measuring local anesthetic binding affinity, and probes the detailed chemistry of local anesthetic-nAChR interactions.

Conformational effects of tetracaine on the nAChR in PC/PA/Chol 3:1:1. We used the same experimental approach to examine the effects of the local anesthetic, tetracaine, on the nAChR reconstituted into four different membrane environments. We first focused on the nAChR in membranes composed of PC/PA/Chol 3:1:1, as the nAChR in this environment fluxes cations in response to agonist binding (Fong and McNamee, 1986). Carb difference spectra recorded from the nAChR reconstituted into PC/PA/Chol 3:1:1 (Fig. 2B, trace *i*), are also similar to those recorded from the nAChR in native membranes (Ryan et al., 1996). These and other data suggest the nAChR in PC/PA/Chol 3:1:1 membranes is stabilized in a functional resting state.

The Carb difference spectrum recorded at 10 μ M concentrations of tetracaine, where tetracaine binding is restricted mainly to its non-competitive inhibitor site in the ion channel pore ($K_D = 1.5 \mu$ M) (Blanchard et al., 1979) is similar to those recorded in the absence of tetracaine (Fig. 2A and 2B), but exhibits subtle *increases* in the intensities of amide I and amide II marker bands that are diagnostic of the resting to desensitized conformational transition ($EC_{50} < 10 \mu$ M; see Table 1 and Table 1S). The most noticeable change is an increase in intensity to the left of the main amide I difference band centered near 1655 cm^{-1} . This increase in intensity leads to a separate positive peak centered near 1663 cm^{-1} (see also Fig. 2, supplemental information) and is

MOL 39008

coupled with an increase in intensity of the amide II difference band near 1545 cm^{-1} . The increased intensity near 1663 cm^{-1} is also evident in spectra recorded at 100 and 200 μM concentrations of tetracaine. The amide I and II increased marker band intensities suggest that tetracaine stabilizes a greater proportion of nAChRs in a conformation that undergoes desensitization upon Carb binding. Although tetracaine is known to reduce acetylcholine binding affinity by binding to its non-competitive inhibitor site and is thus thought to stabilize a resting state (Boyd and Cohen, 1980), the fact that tetracaine increases the intensity near 1663 cm^{-1} to a greater extent than near 1655 cm^{-1} , has been interpreted in terms of the stabilization of a resting-like conformation (for a discussion of this point see Ryan and Baenziger, 1999, Ryan et al., 2002).

In contrast, higher concentrations of tetracaine lead to binding to the neurotransmitter sites ($K_D = 800\text{ }\mu\text{M}$) and a reversal of the spectral changes observed at relatively low concentrations of tetracaine. There are decreases in the intensities of the amide I and amide II marker bands near 1663, 1655 and 1545 cm^{-1} , which are diagnostic of desensitization. As with procaine, the changes in intensity occur concomitant with the appearance of negative tetracaine vibrations, which result from the displacement of tetracaine from the neurotransmitter sites upon Carb binding (dashed line in Fig. 2B). There are decreases in intensity of the putative tryptophan and tyrosine bands near 1620 and 1515 cm^{-1} , respectively, suggesting that tetracaine weakly mimics the quaternary amine-aromatic interactions that normally occur between Carb and binding site residues. Tetracaine shifts the tyrosine vibration up to 1519 cm^{-1} . As with procaine, the intensities and/or frequencies of the $1690/1668\text{ cm}^{-1}$ vibrations observed at high concentrations of tetracaine suggest that tetracaine does not interact with the nAChR residue that normally forms a hydrogen bond with the ester carbonyl of Carb in the esterophilic subsite.

MOL 39008

Above 200 μM , tetracaine binds to the neurotransmitter sites, mimics some of the quaternary amine-aromatic interactions that normally occur between Carb and the nAChR, and appears to stabilize a desensitized conformation of the nAChR. Neurotransmitter site binding reverses the conformational effects that result from tetracaine binding to its non-competitive inhibitor site in the ion channel pore.

Conformational effects of tetracaine on the nAChR in PC. The effects of tetracaine were next examined at the nAChR reconstituted into a membrane that does not stabilize a functional receptor. The nAChR in PC does not flux cations in response to agonist binding (Fong and McNamee, 1986). Carb difference spectra recorded from the nAChR in PC exhibit a pattern of amide I and amide II marker band intensities (Fig. 3B, trace *i*) that is similar to the patterns observed in Carb difference spectra recorded in the presence of desensitizing local anesthetics (Ryan et al., 1996; also see trace *iii* of Fig. 1B, 2B, 4B, and 5B). The nAChR in PC cannot undergo the agonist-induced resting to desensitized conformational transition, possibly because it is already stabilized in a desensitized state. We were interested in testing whether low concentrations of tetracaine ($<50 \mu\text{M}$) could shift the “desensitized” nAChR in PC into a functional resting-like conformation.

Surprisingly, Carb difference spectra recorded from the nAChR in PC membranes in the presence of tetracaine at concentrations up to 50 μM are all essentially identical to those observed in the absence of tetracaine (Fig. 3B, traces *i* and *ii*). Superimposition of the spectra shows that no dose dependent increase in intensity of any of the amide I or amide II difference bands indicative of desensitization can be detected (data not shown, but see Fig. 3 of supplemental information). Tetracaine cannot induce a conformational shift towards a resting or resting-like conformation when the nAChR is reconstituted into PC.

MOL 39008

At concentrations of tetracaine above 200 μM , negative tetracaine vibrations suggestive of tetracaine binding to the neurotransmitter sites are observed (dashed line in Fig. 3B). These bands first appear at concentrations of tetracaine similar to those at which they appear in difference spectra recorded from the nAChR in PC/PA/Chol 3:1:1 membranes. At higher concentrations of tetracaine, however, the negative tetracaine bands are consistently weaker in the difference spectra recorded from the nAChR in PC than in PC/PA/Chol 3:1:1. Even at 2 mM tetracaine, the amount of tetracaine displaced upon Carb binding to the nAChR reaches only ~50% of that observed at 800 μM tetracaine in PC/PA/Chol 3:1:1. Further, tetracaine has minimal if any effect on the intensities of either the putative tryptophan or tyrosine vibrations. The tyrosine vibration, which in PC membranes occurs near 1517 cm^{-1} , does not shift up in frequency upon tetracaine binding (see Fig. 6). Note also that the increase in intensity of the tyrosine vibration in PC membranes is weaker than in PC/PA/Chol 3:1:1 membranes. These results, which are discussed in more detail below, suggest an altered binding of tetracaine to the neurotransmitter sites in PC versus PC/PA/Chol 3:1:1 membranes.

Conformational effects of tetracaine on the nAChR in PC/PA 3:2 membranes. The effects of tetracaine were next examined with the nAChR reconstituted into PC/PA 3:2 membranes. The Carb difference spectrum recorded in the absence of tetracaine exhibits a pattern of amide I and II marker bands that is close, but not identical to that observed in both PC/PA/Chol 3:1:1 and native membranes (Fig. 4B, trace *i*) (Baenziger et al., 2000; daCosta et al., 2002). PA alone in a PC membrane is thus effective at stabilizing the nAChR in a functional state that undergoes Carb induced desensitization (Baenziger et al., 2000).

Similar to the data obtained with the nAChR in PC/PA/Chol 3:1:1 membranes, concentrations of tetracaine up to 50 μM where binding is restricted to its non-competitive

MOL 39008

inhibitor site, lead to reproducible increases in the intensities of amide I and II marker bands indicative of desensitization (Fig. 4). Specifically, there are slight increases in intensity near 1655 and 1545 cm^{-1} , and the appearance of new positive intensity near 1663 cm^{-1} ($\text{EC}_{50} < 10 \mu\text{M}$; Table 1 and Table 1S). The increase in intensity near 1663 cm^{-1} is clearly visible in spectra recorded at 5 μM tetracaine, and remains evident as a distinct peak in spectra recorded at 10, 25, 50, and 100 μM concentrations of tetracaine (see Fig. 4 of supplemental information). Tetracaine binding to its non-competitive inhibitor site thus favors a resting-like conformation. The presence of PA alone in a PC membrane is sufficient to impart sensitivity to tetracaine binding at its non-competitive inhibitor site.

At higher concentrations, tetracaine reverses the conformational effects that result from non-competitive inhibitor site(s) binding. There is a reduction in the intensities of all the amide I and II marker bands indicative of the resting to desensitized conformational transition, the appearance of vibrational bands suggestive of binding to the neurotransmitter sites, and a decrease in the intensities of bands near 1620 and 1515 cm^{-1} , suggesting that tetracaine mimics the quaternary amine-aromatic interactions that occur between Carb and binding site residues. Tetracaine shifts the frequency of the tyrosine vibration up to near 1519 cm^{-1} . Tetracaine binds to the neurotransmitter site and likely stabilizes the desensitized state.

As with the nAChR in PC/PA/Chol 3:1:1, the conformational effects of tetracaine at the nAChR in PC/PA 3:2 membranes are dependent upon the site of tetracaine binding. The presence of PA in the PC membrane is sufficient to stabilize the nAChR in a state that responds fully to tetracaine's sensitizing and desensitizing actions.

Conformational effects of tetracaine on the nAChR in PC/Chol 3:2 membranes. Finally, the effects of tetracaine were examined on the nAChR reconstituted into the binary lipid mixture

MOL 39008

PC/Chol 3:2. In the absence of tetracaine, Carb difference spectra recorded from the nAChR in PC/Chol 3:2 exhibit a pattern of amide I and II marker band intensities intermediate between that observed in PC/PA/Chol 3:1:1 and pure PC membranes (Fig. 5B, trace *i*) (Baenziger et al., 2000; daCosta et al., 2002). The presence of Chol in a PC membrane thus stabilizes the nAChR in a functional state, but the proportions of functional receptors is lower than that observed in PC/PA/Chol 3:1:1 and PC/PA 3:2 membranes.

In contrast to the data obtained for the nAChR in PC/PA 3:2 membranes, Carb difference spectra recorded from the nAChR in PC/Chol 3:2 in the absence or presence of concentrations of tetracaine up to 50 μ M are all essentially identical (Fig. 5 and Fig. 5 of supplemental information). Superimposition of the spectra (data not shown) does not reveal any dose dependent changes in difference band intensity that can be attributed to an increase in the number of receptors stabilized in a resting state. Unlike PA, the presence of Chol in a reconstituted PC membrane does not appear to impart on the nAChR an ability to respond to tetracaine binding to its non-competitive inhibitor site.

Concentrations of tetracaine above 200 μ M, however, lead to spectral changes similar to those observed in both PC/PA/Chol 3:1:1 and PC/PA 3:2 membranes. These include a decrease in the intensities of the amide I and II marker bands suggestive of the stabilization of a desensitized state, the appearance of negative tetracaine bands suggestive of tetracaine binding to the neurotransmitter sites, and a decrease in the intensities of bands that reflect the formation of physical interactions between Carb and binding site aromatic residues. As in PC membranes alone, tetracaine has minimal effect on the frequencies of the putative binding-site tyrosine vibration, which occurs near 1517 cm^{-1} . At these concentrations, tetracaine binds to the

MOL 39008

neurotransmitter site, mimics some of the Carb-nAChR quaternary amine-aromatic interactions, and induces a conformational shift towards the desensitized state.

Agonist binding to the nAChR in PC and PC/PA/Chol 3:1:1 membranes. There are several explanations for why tetracaine has no conformational effect at its non-competitive inhibitor site of the nAChR in PC and PC/Chol 3:2 membranes. One possibility is that these membranes favor a single conformation of the nAChR so strongly that binding of tetracaine has minimal effect on the number of receptors in either the resting or desensitized conformations. A second possibility is that the presence of PA enhances the partitioning of the positively charged tetracaine into the lipid bilayer (Table 2). If tetracaine accesses to its non-competitive inhibitor site in the channel pore from the bilayer, then enhanced partitioning in the presence of PA would increase the local tetracaine concentration and thus increase apparent efficacy of tetracaine action at its non-competitive inhibitor site.

An alternative explanation, however, is suggested by the membrane and local anesthetic dependent variations in the intensities/frequencies of the putative binding site tyrosine and tryptophan residues, which are noted throughout the above text. These intensity/frequency variations are highlighted for the nAChR in PC and PC/PA/Chol 3:1:1 membranes in Figure 6. They suggest subtle lipid-dependent differences in the structures of the neurotransmitter binding sites of the nAChR, even in the presence of bound Carb. The agonist-bound neurotransmitter binding sites of the nAChR in PC and possibly PC/Chol 3:2 membranes may adopt structures distinct from the agonist desensitized structures of the neurotransmitter sites in PC/PA/Chol 3:1:1 and PC/PA 3:2 membranes (see Discussion). Lipids may alter nAChR function by mechanisms more complex than modulation of a simple equilibrium between activatable resting and non- activatable desensitized states.

To test whether the lipid and local anesthetic dependent variations in intensity/frequency of the tyrosine and tryptophan vibrations reflect variations in binding site structure, we qualitatively probed the affinity of agonist binding to the nAChR in PC/PA/Chol 3:1:1 versus PC membranes. Infrared difference spectra are sensitive to affinity because the absolute intensities of difference bands reflect the number of nAChRs that bind Carb, which depends on both the number of molecules of nAChR in the sample that are probed by the infrared light and the proportion of these that bind agonist at the utilized agonist concentration. As the nAChR films extend beyond the penetration depth of the infrared evanescent wave (i.e. the infrared light samples only a small proportion of the entire sample; see Figure 1 of supplemental information), the number of receptors sampled by the evanescent wave in each experiment is relatively constant. The relative intensities of the difference bands from one spectrum to another thus provide a quick measure of the proportion of receptors in each sample that bind agonist at a given agonist concentration.

As a control, we first recorded difference spectra from the nAChR in PC/PA/Chol 3:1:1 versus PC membranes using concentrations of Carb, 50 μ M and 250 μ M, that are well above the K_D for Carb binding the desensitized nAChR in native membranes (K_D = 25 nM; for the resting state, K_D = 30 μ M; Boyd and Cohen, 1980). Although the pattern of vibrations due to the conformational change in spectra recorded from the nAChR in PC/PA/Chol 3:1:1 versus PC membranes are different, the intensities of a few key vibrations including the bound Carb vibrations near 1724 cm^{-1} and the protein vibrations near 1690 and 1620 cm^{-1} are similar in difference spectra recorded from the nAChR in both membranes and at 50 and 250 μ M Carb. These data show that the amount of Carb binding to the nAChR in both membrane environments is essentially equivalent at 50 and 250 μ M concentrations of Carb. They also show the

MOL 39008

reproducibility of the band intensities in difference spectra recorded from the nAChR in PC versus PC/PA/Chol 3:1:1 membranes.

Carb difference spectra recorded at much lower concentrations could provide insight into the relative affinities of the nAChR in both PC and PC/PA/Chol 3:1:1 membranes for Carb, but at concentrations in the nM range, insufficient amounts of Carb are added to saturate the number of Carb binding sites in each membrane film (≈ 2 nmoles binding sites), regardless of whether the concentration of Carb is above the K_D . We therefore examined the binding of the agonist analog, tetramethylamine (TMA), which binds the nAChR with lower affinity (equilibrium binding affinity is ≈ 0.5 mM; Akk and Auerbach, 1996).

Difference spectra recorded using 10 μ M and 1 mM concentrations of TMA exhibit marked differences in intensity for the nAChR reconstituted in PC/PA/Chol 3:1:1 versus PC membranes, and at the two concentrations studied. TMA difference spectra recorded from the nAChR in PC/PA/Chol 3:1:1 membranes at TMA concentrations of 10 μ M and 1 mM exhibit difference bands indicative of both TMA binding and the resting to desensitized conformational transition, but at 10 μ M TMA the absolute intensities of the bands are roughly 30% of those observed in the spectra recorded at 1 mM TMA. Higher concentrations of TMA did not lead to additional levels of TMA binding. In contrast, the 10 μ M TMA difference spectra recorded from the nAChR in PC membranes do not exhibit any difference bands detectable above the level of noise showing that TMA does not bind appreciably to the nAChR in PC at this concentration. Protein difference bands are observed in difference spectra recorded using 1 mM TMA concentrations, most notably at 1620 cm^{-1} , but these are less than 25% as intense as those observed in the TMA difference spectra recorded from the nAChR in PC/PA/Chol 3:1:1 membranes at the same concentration of TMA. The weak difference band intensities show that

MOL 39008

much less TMA binds to the nAChR in PC versus PC/PA/Chol 3:1:1 membranes at these equivalent concentrations of TMA. The nAChR in PC has a lower affinity for the agonist TMA than the nAChR in PC/PA/Chol 3:1:1 membranes and thus has a neurotransmitter binding site structure that differs from the structure of the TMA-desensitized neurotransmitter binding site in PC/PA/Chol 3:1:1 membranes.

MOL 39008

Discussion

Our data show that membrane lipid composition influences tetracaine action at the nAChR. Concentrations of tetracaine ($<50\ \mu\text{M}$) consistent with non-competitive inhibitor site binding and the consequent stabilization of a resting conformation of the nAChR in native membranes also stabilize the nAChR in a resting or resting-like state in membranes composed of PC/PA 3:2 and PC/PA/Chol 3:1:1. In contrast, similar concentrations of tetracaine have no effect on nAChR conformational equilibria with the nAChR in PC and PC/Chol 3:2 membranes. These observations are significant because increasing evidence indicates that neuronal nAChRs are associated with membrane rafts (Bruses et al., 2001; Roth and Berg, 2003; Zhu et al., 2006). As the lipid composition in rafts differs from that of the bulk membrane, our findings indicate that drug action at the nAChR, and other membrane proteins, could vary depending on whether the receptor is located in raft or non-raft environments. Changes in lipid composition during development and/or in disease states could alter drug action *in vivo*. Mechanistic studies of drug action at membrane protein targets must therefore take into account the membrane environment in which the target is imbedded.

The data also provide insight into the mechanisms by which lipids and local anesthetics influence nAChR function. Typically, the conformational effects of both lipids and local anesthetics are interpreted in terms of a two state model. In native membranes, the natural equilibrium between functional resting and non-functional desensitized conformations favors the resting state ($\sim 80\%$ resting). In PC membranes, the nAChR does not flux cations or undergo an agonist induced conformational change, consistent with the stabilization of a desensitized nAChR. A desensitized nAChR is also suggested by the labeling pattern of the nAChR with the hydrophobic probe, 3-trifluoromethyl-3-(*m*-[^{125}I]iodophenyl) diazirine (daCosta et al., 2002).

MOL 39008

Increasing concentrations of PA and/or Chol in a PC membrane stabilize an increasing number of receptors in a resting conformation that undergoes conformational change upon agonist binding. PA is more effective than Chol at stabilizing a resting state. The data suggest that lipids might influence nAChR function by modulating the conformational equilibrium between resting and desensitized receptors.

Tetracaine binds preferentially to a non-competitive inhibitor site(s) on the resting nAChR in native membranes and shifts the natural equilibrium between resting and desensitized receptors in favor of the resting state. As noted, tetracaine has a similar effect on the nAChR in both PC/PA 3:2 and PC/PA/Chol 3:1:1 membranes. The natural equilibrium between resting and desensitized receptors thus exists in PA containing membranes and is modulated by tetracaine binding. If the natural equilibrium between resting and desensitized nAChRs also exists in PC/Chol 3:2 and PC membranes, but with the equilibrium shifted to varying degrees towards the desensitized state, we should still see a shift in conformation towards the resting nAChR at concentrations consistent with tetracaine binding to its non-competitive inhibitor site. So why does tetracaine not stabilize a resting nAChR in PC and PC/Chol 3:2 membranes?

One possibility is that the natural equilibrium between the two conformations is so strongly shifted in favor of either the resting or desensitized conformations that tetracaine binding has little effect. The activation energy for conversion between the two states could also be so large that the kinetics of conformational change are too slow to be detected in our experiments (minutes time scale). Both explanations can explain the lack of tetracaine action at its non-competitive inhibitor site on the nAChR in PC. For the nAChR in PC/Chol 3:2, however, a proportion of the nAChRs are stabilized in the absence of tetracaine in a conformation that undergoes agonist-induced desensitization in response to Carb binding. Neither a dramatic

MOL 39008

increase in the stability of the resting or desensitized nAChRs nor a dramatic increase in the activation energy between the two conformations are thus compatible PC/Chol 3:2 data.

A second possibility is that the absence of the negatively charged PA reduces the partitioning of the positively charged tetracaine into the PC and PC/Chol 3:2 lipid bilayers (Table 2). If tetracaine accesses its non-competitive inhibitor site in the channel pore from the membrane, the low membrane concentrations of tetracaine in PC and PC/Chol 3:2 membranes would reduce the effective EC_{50} for non-competitive inhibitor site(s) action. Even a modest decrease in apparent affinity might increase the effective EC_{50} to a value above the EC_{50} for action at the neurotransmitter sites. In such a case, the conformational effects of tetracaine in PC and PC/Chol 3:2 would be dominated by neurotransmitter site binding, as is observed with procaine (Fig. 1). Note that while direct access to the channel pore from the lipid bilayer is not evident in the atomic resolution model of the nAChR (Unwin, 2005), internal breathing motions might create such a pathway.

An altered partitioning into the membrane environment, however, cannot account for the subtle membrane dependent variations detected in the binding of both Carb and tetracaine to the neurotransmitter sites. The binding of Carb leads to an increase in tyrosine vibrational intensity, likely due to the formation of quaternary amine cation-tyrosine π -electron interactions, but the affected tyrosine(s) in PC/PA/Chol 3:1:1 and PC/PA 3:2 vibrate at $\sim 1515\text{ cm}^{-1}$, whereas in PC and PC/Chol 3:2 it(they) vibrate near 1517 cm^{-1} . The distinct tyrosine vibrational frequencies suggest distinct local environments surrounding the tyrosine(s) in PC/PA/Chol 3:1:1 and PC/PA 3:2 versus PC and PC/Chol 3:2 membranes. For example, the affected tyrosine(s) may hydrogen bond to adjacent residues more or less strongly in PC/PA/Chol 3:1:1 and PC/PA 3:2 than in PC and PC/Chol 3:2. Note that the binding of Carb to the nAChR also leads to a much larger

MOL 39008

increase in tyrosine vibrational intensity in PC/PA/Chol 3:1:1, PC/PA 3:2, and PC/Chol 3:2 than in PC membranes (Fig. 6) suggesting that Carb interacts more effectively with the neurotransmitter site tyrosine(s) in the former three membranes. In this regard, the neurotransmitter binding site of the nAChR in PC/Chol 3:2 appears to resemble more closely the binding site in PC/PA/Chol 3:1:1 and PC/PA 3:2 membranes.

Tetracaine concentrations consistent with neurotransmitter site binding lead to an appreciable decrease in intensity of tyrosine and tryptophan residues near ~ 1515 and 1620 cm^{-1} , respectively, for the nAChR in PC/PA/Chol 3:1:1, PC/PA 3:2, and PC/Chol 3:2 membranes, but not for the nAChR in PC membranes. The decreases in intensity suggests that tetracaine forms similar, but weaker, quaternary amine-aromatic interactions with the nAChR prior to Carb binding when the nAChR is in PC/PA/Chol 3:1:1, PC/PA 3:2, and PC/Chol 3:2, but not in PC membranes. Tetracaine also leads to a shift up in frequency of the weak tyrosine vibration from 1515 to 1519 cm^{-1} with the nAChR in PC/PA/Chol 3:1:1 and PC/PA 3:2 membranes, while it has little effect on the frequencies of the same vibrations in spectra recorded from the nAChR in PC and PC/Chol 3:2 membranes.

Collectively, these results suggest altered interactions between Carb/tetracaine and neurotransmitter site tyrosine and tryptophan residues, as a result of altered structures of the neurotransmitter sites in PC versus PC/Chol 3:2 versus PC/PA/Chol 3:1:1 and PC/PA 3:2 membranes. Further, we show qualitatively that the nAChR has a weaker affinity for the agonist analog, TMA, in PC versus the TMA desensitized nAChR in PC/PA/Chol 3:1:1. This confirms that the noted changes in tyrosine and tryptophan vibrations reflect changes in neurotransmitter site structure and highlights the utility of FTIR for monitoring the subtle features of membrane receptor-drug interactions. More importantly, they confirm that the TMA bound

MOL 39008

neurotransmitter sites of the nAChR in PC membranes are not equivalent in structure to the TMA desensitized binding sites of the nAChR in PC/PA/Chol 3:1:1 and PC/PA 3:2 membranes.

Most studies suggest that lipids influence nAChR function by modulating the equilibrium between resting and desensitized states with the non-activatable nAChR in PC reflecting a desensitized or desensitized-like conformation. Our data show that the neurotransmitter sites of the nAChR in PC are not desensitized in the presence of bound agonist. One possible explanation is that the nAChR in PC is locked in a resting conformation that does not undergo agonist-induced conformational change (Rankin et al., 1997). The nAChR in PC, however, exhibits a chemical labeling pattern of the channel pore that is not consistent with a resting nAChR (daCosta et al, 2002). The hydrogen exchange kinetics and thermal denaturation of the nAChR in PC are also not consistent with a resting conformation (Methot et al., 1995; daCosta et al, 2005). The different lipid environments studied here likely influence local anesthetic action by stabilizing unique conformations that have altered sensitivities to local anesthetic action.

Conclusions

This study illustrates the complex interplay that can exist between lipid composition and drug action, and highlight some of the different mechanisms by which lipids might influence drug action at membrane protein targets. Changes in lipid composition could influence the access of lipophilic drugs to membrane protein sites by altering the partitioning of drugs into the lipid bilayer. Changes in lipid composition may also stabilize membrane protein targets in different conformations that are more or less responsive to drug action. In this regard, it is important to note that although we have studied relatively dramatic changes in lipid environment, even subtle changes in nicotinic receptor gated channel function can have serious pathological

MOL 39008

consequences (Engel and Sine, 2006). Subtle changes in lipid composition *in vivo* could alter membrane protein function and thus drug action. Understanding drug action at integral membrane protein receptors, in general, may require understanding the conformational properties of membrane proteins in varying lipid environments.

MOL 39008

References

- Akk G and Auerbach A (1996) Inorganic, monovalent cations compete with agonists for the transmitter binding site of nicotinic acetylcholine receptors. *Biophys. J.* **70**:2652-2658.
- Allen JA, Halverson-Tamboli RA & Rasenick MM (2007) Lipid raft microdomains and neurotransmitter signaling. *Nat. Rev. Neuroscience* **8**:128-140
- Arias HR, Bhumireddy P and Bouzat C (2006) Molecular mechanisms and binding site locations for noncompetitive antagonists of nicotinic acetylcholine receptors. *Int. J. Biochem. Cell Biol.* **38**:1254-1276.
- Baenziger JE and Chew JP (1997) Desensitization of the nicotinic acetylcholine receptor mainly involves a structural change in solvent-accessible regions of the polypeptide backbone. *Biochemistry* **36**:3617-3624.
- Baenziger JE, Miller, KW and Rothschild KJ (1992) Incorporation of the nicotinic acetylcholine receptor into planar multilamellar films: characterization by fluorescence and Fourier transform infrared difference spectroscopy. *Biophys. J.* **61**:983-992
- Baenziger JE, Morris ML, Darsaut TE and Ryan SE (2000) Effect of membrane lipid composition on the conformational equilibria of the nicotinic acetylcholine receptor. *J. Biol. Chem.* **275**:777-784.
- Baenziger JE, Miller KW and Rothschild KJ (1993) Fourier transform infrared difference spectroscopy of the nicotinic acetylcholine receptor: evidence for specific protein structural changes upon desensitization. *Biochemistry* **32**:5448-5454.
- Barrantes FJ (2004) Structural basis for lipid modulation of nicotinic acetylcholine receptor function. *Brain. Res. Rev.* **47**:71-95.

MOL 39008

Barrantes FJ (2002) Lipid matters: nicotinic acetylcholine receptor-lipid interactions (Review).

Mol. Membr. Biol. **19**:277-284.

Barth A (2000) The infrared absorption of amino acid side chains. *Prog. Biophys. Mol. Biol.*

74:141-173.

Blanchard SG, Elliott J and Raftery MA (1979) Interaction of local anesthetics with Torpedo californica membrane-bound acetylcholine receptor. *Biochemistry* **18**:5880-5885.

Boyd ND and Cohen JB (1980) Kinetics of binding of [3H]acetylcholine and [3H]carbamoylcholine to Torpedo postsynaptic membranes: slow conformational transitions of the cholinergic receptor. *Biochemistry* **19**:5344-5353.

Brudler R, Rammelsberg R, Woo TT, Getzoff ED, and Gerwert K (2001) Structure of the I1 early intermediate of photoactive yellow protein by FTIR spectroscopy. *Nat. Struct. Biol.* **8**:265-270.

Bruses JL, Chauvet N and Rutishauser U (2001) Membrane lipid rafts are necessary for the maintenance of the (alpha)7 nicotinic acetylcholine receptor in somatic spines of ciliary neurons. *J. Neurosci.* **21**:504-512.

daCosta CJB, Kaiser DE, and Baenziger JE (2005) Role of glycosylation and membrane environment in nicotinic acetylcholine receptor stability. *Biophys. J.* **88**:1755-1764.

daCosta CJB, Ogrel AA, McCardy EA, Blanton MP and Baenziger JE (2002) Lipid-protein interactions at the nicotinic acetylcholine receptor. A functional coupling between nicotinic receptors and phosphatidic acid-containing lipid bilayers. *J. Biol. Chem.* **277**:201-208.

Sine SM, and Engel AG (2006) Recent advances in Cys-loop receptor structure and function.

Nature **440**: 448-455.

MOL 39008

Fong TM and McNamee MG (1986) Correlation between acetylcholine receptor function and structural properties of membranes. *Biochemistry* **25**:830-840.

Hill DG and Baenziger JE (2006) The net orientation of nicotinic receptor transmembrane alpha-helices in the resting and desensitized states. *Biophys. J.* **91**:705-714.

Jackson M and Mantsch HH (1995) The use and misuse of FTIR spectroscopy in the determination of protein structure. *Crit. Rev. Biochem. Mol. Biol.* **30**:95-120.

Krodel EK, Beckman RA and Cohen JB (1979) Identification of a local anesthetic binding site in nicotinic post-synaptic membranes isolated from *Torpedo marmorata* electric tissue. *Mol. Pharmacol.* **15**:294-312.

Kötting C and Gerwert K. (2005) Proteins in action monitored by time-resolved FTIR spectroscopy. *ChemPhysChem.* **6**:881-888.

Lee AG (2004) How lipids affect the activities of integral membrane proteins (review). *Biochim. Biophys. Acta* **1666**:62-87

Lester HA, Dibas MI, Dahan DS, Leite JF and Dougherty DA (2004) Cys-loop receptors: new twists and turns. *Trends. Neurosci.* **27**:329-336.

McMahon HT and Gallop JL (2005) Membrane curvature and mechanisms of dynamic cell membrane remodelling. *Nature* **438**:590-596

Miller KW (2002) The nature of sites of general anaesthetic action (review). *Br. J. Anaesth.* **89**:17-31.

Methot N, Demers CN, and Baenziger JE (1995) Structure of both the ligand- and lipid-dependent channel-inactive states of the nicotinic acetylcholine receptor probed by FTIR spectroscopy and hydrogen exchange. *Biochemistry* **34**:15142-15149.

MOL 39008

Overington JP, Al-Lazikani B, and Hopkins AL (2006) How many drug targets are there? *Nat. Rev. Drug Discov.* **5**:993-996.

Romsicki Y and Sharom FJ (1999) The membrane lipid environment modulates drug interactions with the P-glycoprotein multidrug transporter. *Biochemistry* **38**:6887-6896.

Roth AL and Berg DK (2003) Large clusters of alpha7-containing nicotinic acetylcholine receptors on chick spinal cord neurons. *J. Comp. Neurol.* **465**:195-204.

Rankin SE, Addona GH, Kloczewiak MA, Bugge B, and Miller KW (1997) The cholesterol dependence of activation and fast desensitization of the nicotinic acetylcholine receptor. *Biophys. J.* **73**:2446-2455.

Ryan SE, Hill DG and Baenziger JE (2002) Dissecting the chemistry of nicotinic receptor-ligand interactions with infrared difference spectroscopy. *J. Biol. Chem.* **277**:10420-10426

Ryan SE and Baenziger JE (1999) A structure-based approach to nicotinic receptor pharmacology. *Mol. Pharmacol.* **55**:348-355.

Ryan SE, Demers CN, Chew JP and Baenziger JE (1996) Structural effects of neutral and anionic lipids on the nicotinic acetylcholine receptor. An infrared difference spectroscopy study. *J. Biol. Chem.* **271**:24590-24597.

Sine SM and Engel AG (2006) Recent advances in Cys-loop receptor structure and function. *Nature* **440**:448-455.

Szabo G, Dolganiuc A, Dai Q and Pruett SB (2007) TLR4, Ethanol, and Lipid Rafts: A New Mechanism of Ethanol Action with Implications for other Receptor-Mediate Effects (Review). *J. Immunol.* **178**:1243-1249

MOL 39008

Unwin N (2005) Refined structure of the nicotinic acetylcholine receptor at 4Å resolution. *J. Mol. Biol.* **346**:967-989

Vogel R and Siebert F (2003) Fourier transform IR spectroscopy study for new insights into molecular properties and activation mechanisms of visual pigment rhodopsin. *Biopolymers* **72**:133-148.

Zhong W, Gallivan JP, Zhang Y, Lintong Li, Lester HA and Dougherty DA (1998) From *ab initio* quantum mechanics to molecular neurobiology: A cation- π binding site in the nicotinic receptor. *Proc. Natl. Acad. Sci. USA* **95**:12088-12093.

Zhu D, Xiong WC and Mei L (2006) Lipid Rafts Serve as a Signaling Platform for Nicotinic Acetylcholine Receptor Clustering. *J. Neurosci.* **26**:4841-4851

MOL 39008

Footnotes

This work was supported by grants from the Canadian Institutes of Health Research to J.E.B. and a National Science and Engineering Council of Canada graduate scholarship to S.E.R.

Address correspondence to: John Baenziger, Department of Biochemistry, Microbiology, and Immunology, University of Ottawa, 451 Smyth Road, Ottawa, Ontario, Canada, K1H 8M5. e-mail: jebaenz@uottawa.ca

MOL 39008

Figure Legends

Figure 1: The conformational effects of procaine at the nAChR in PC/PA/Chol 3:1:1. **a)** Stacked plot of Carb difference spectra recorded from the nAChR in the presence of (from top to bottom) 0, 0.1 mM, 0.5 mM, 1 mM, 2 mM, 4 mM, and 6 mM procaine. **b)** Representative spectra recorded at **i)** 0, **ii)** 0.1, and **iii)** 6 mM procaine. The bottom spectrum **iv)** is a buffer subtracted spectrum of procaine in solution. The dashed line at 1605 cm^{-1} indicates the negative procaine vibrations in the Carb difference spectra. **c)** Dose response curves are for the changes in protein backbone conformation indicative of the formation of a desensitized state (solid squares, monitored at 1655 cm^{-1}), binding of procaine to the neurotransmitter sites (open squares, monitored at 1605 cm^{-1}), and the formation of local anesthetic-nAChR binding site physical interactions (open circles, monitored at 1515 cm^{-1}), as discussed in the text.

Figure 2: The conformational effects of tetracaine at the nAChR in PC/PA/Chol 3:1:1. **a)** Stacked plot of Carb difference spectra recorded from the nAChR in the presence of (from top to bottom) 0, 10 μM , 100 μM , 200 μM , 400 μM , 600 μM , and 800 μM tetracaine. **b)** Representative spectra recorded at **i)** 0, **ii)** 10 μM , and **iii)** 800 μM tetracaine. The bottom spectrum **iv)** is a buffer subtracted spectrum of tetracaine in solution. The dashed line at 1605 cm^{-1} indicates the tetracaine vibrations in the Carb difference spectra. **c)** Dose response curves are as described in Fig. 1, except that bands due to the increase in intensity of the vibration near 1663 cm^{-1} are also plotted (solid triangles). Bands due to the binding of tetracaine to the neurotransmitter sites (open squares) are also monitored at 1605 cm^{-1} . Note that the fit binding curves for the open circles and filled squares overlap.

Figure 3: The conformational effects of tetracaine at the nAChR in PC. **a)** Stacked plot of Carb difference spectra recorded from the nAChR in the presence of (from top to bottom) 0, 5 μM , 10 μM , 50 μM , 100 μM , 200 μM , 400 μM , 600 μM , 800 μM , 1 mM, and 2 mM tetracaine. **b)** Representative spectra recorded at **i)** 0, **ii)** 10 μM , and **iii)** 800 μM tetracaine. The bottom spectrum **iv)** is a buffer subtracted spectrum of tetracaine in solution. The dashed line indicates the tetracaine vibrations in the Carb difference spectra. **c)** The dose response curve is for the binding of tetracaine to the neurotransmitter sites (open squares, monitored at 1605 cm^{-1}). No dose dependent conformational changes were detected.

Figure 4: The conformational effects of tetracaine at the nAChR in PC/PA 3:2. **a)** Stacked plot of Carb difference spectra recorded from the nAChR in the presence of (from top to bottom) 0, 5 μM , 10 μM , 25 μM , 50 μM , 100 μM , 200 μM , 300 μM , 400 μM , and 600 μM tetracaine. **b)** Representative spectra recorded at **i)** 0, **ii)** 10 μM , and **iii)** 600 μM tetracaine. The bottom spectrum **iv)** is a buffer subtracted spectrum of tetracaine in solution. The dashed line indicates the tetracaine vibrations in the Carb difference spectra. **c)** Dose response curves are as described in Fig. 2.

MOL 39008

Figure 5: The conformational effects of tetracaine at the nAChR in PC/Chol 3:2. **a)** Stacked plot of Carb difference spectra recorded from the nAChR in the presence of (from top to bottom) 0, 10 μ M, 50 μ M, 100 μ M, 200 μ M, 300 μ M, 400 μ M, 500 μ M, 600 μ M, and 800 μ M tetracaine. **b)** Representative spectra recorded at **i)** 0, **ii)** 10 μ M, and **iii)** 800 μ M tetracaine. The bottom spectrum **iv)** is a buffer subtracted spectrum of tetracaine in solution. The dashed line indicates the tetracaine vibrations in the Carb difference spectra. **c)** Dose response curves are as described in Fig. 2.

Figure 6: Vibrational changes in aromatic residues upon binding of tetracaine to the neurotransmitter sites of the nAChR. **a)** Overlapped Carb difference spectra recorded at 0 μ M (solid black lines) and 800 μ M (dashed grey lines) tetracaine from the nAChR in PC/PA/Chol 3:1:1 (top two traces) and PC (bottom two traces) membranes. The grey shaded regions highlight putative bands due to binding site tryptophan (1620 cm^{-1}) and tyrosine residues (1515-1519 cm^{-1}). The dashed line is at 1517 cm^{-1} . Note that the tryptophan vibrations near 1620 cm^{-1} in difference spectra recorded in the absence and presence of tetracaine do not overlap due to intensity changes near 1640 cm^{-1} .

Figure 7: Carb (A) and TMA (B) difference spectra recorded from the nAChR in PC/PA/Chol 3:1:1 (traces i and ii in both A and B) and PC (traces iii and iv in both A and B) membranes. The Carb difference spectra in A were recorded using 50 μ M (traces i and iii) and 250 μ M (traces ii and iv) concentrations of Carb. The TMA difference spectra in B were recorded using 10 μ M (traces i and iii) and 1 mM (traces ii and iv) concentrations of TMA. Dark shading denotes amide I and amide II bands that reflect the backbone conformational change associated with desensitization. The lighter shading highlighted by the black dashed lines indicates the vibrational bands attributed to Carb at 1724 cm^{-1} (A) and TMA at 1484 cm^{-1} (B). At 1 mM TMA, the TMA vibrations reflect primarily free TMA in solution.

MOL 39008

Table 1

Pharmacological Data for the Spectral Effects that result from Local Anesthetic Action at the nAChR

Membrane	EC ₅₀ (μM) ¹			
	Conformational Change to R ²	Conformational Change to D ³	Anesthetic Binding ⁴	Anesthetic-nAChR Physical Interactions ⁵
PC (with tetracaine)	NA ⁶	ND ⁷	216±3	ND
PC/Chol 3:2 (with tetracaine)	NA	269±54	204±32	136±37
PC/PA 3:2 (with tetracaine)	1.6	230±16	188±130	181±22
PC/PA/Chol 3:1:1 (with tetracaine)	5.9	365±33	519±96	297±56
PC/PA/Chol 3:1:1 (with procaine)	NA	542±173	588±52	588±88

¹ Each reported EC₅₀ (except for data in the first column) is the average of two EC₅₀ values obtained by monitoring two different vibrational bands (±standard deviation with n=2). Note that each data point in each dose-response curve is taken from an average of 30 to 60 difference spectra/individual difference experiments. See Materials and Methods

² reflects the conformational shift to a resting-like conformation

³ reflects the conformational shift to a desensitized conformation

⁴ reflects local anesthetic binding to the neurotransmitter sites

⁵ reflects the formation of physical interactions between the local anesthetic and neurotransmitter binding site aromatic residues, ⁶ NA; Not applicable, ⁷ ND; Not determined

MOL 39008

Table 2
Partition Coefficients¹ for Tetracaine in Lipid Bilayers

Lipid	[Tetracaine] ² (μ M)	Partition Coefficient ³
PC	41	140 \pm 3
PC/Chol 3:2 (mol:mol)	74	38 \pm 3
PC/PA 3:2 (mol:mol)	16	510 \pm 23
PC/PA/Chol 3:1:1 (mol:mol:mol)	19	440 \pm 40

¹ Partition Coefficient = $((C_O - C_S) \times W_B) / (C_S \times W_L)$ where C_O is the initial concentration of tetracaine (100 μ M), C_S is the final concentration of tetracaine in the supernatant, W_B is the weight of the buffer, and W_L is the weight of the lipid (10 mg/ml).

²Concentration of tetracaine remaining free in solution, C_S

³data are \pm the standard deviation with n=2

Figure 1

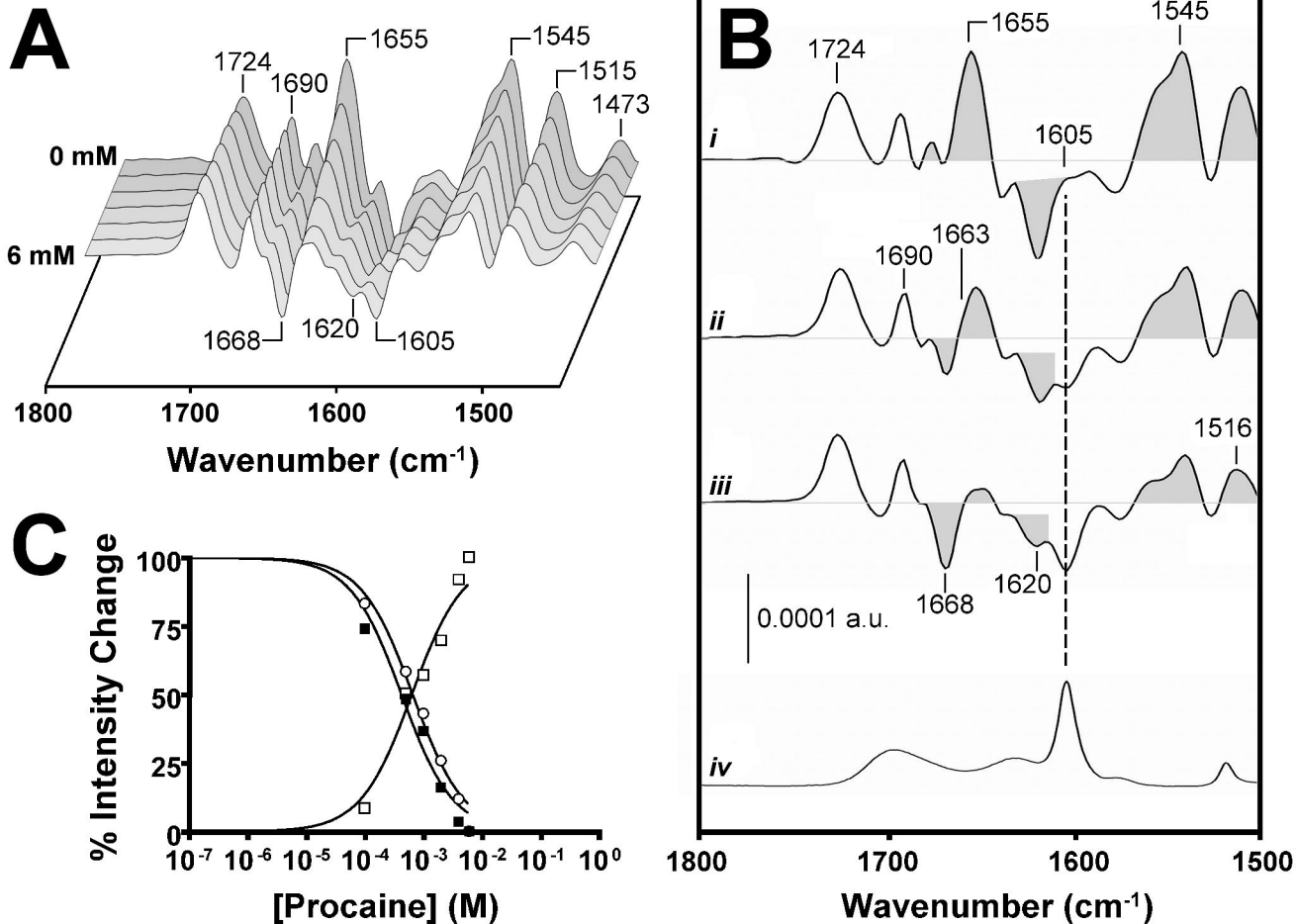


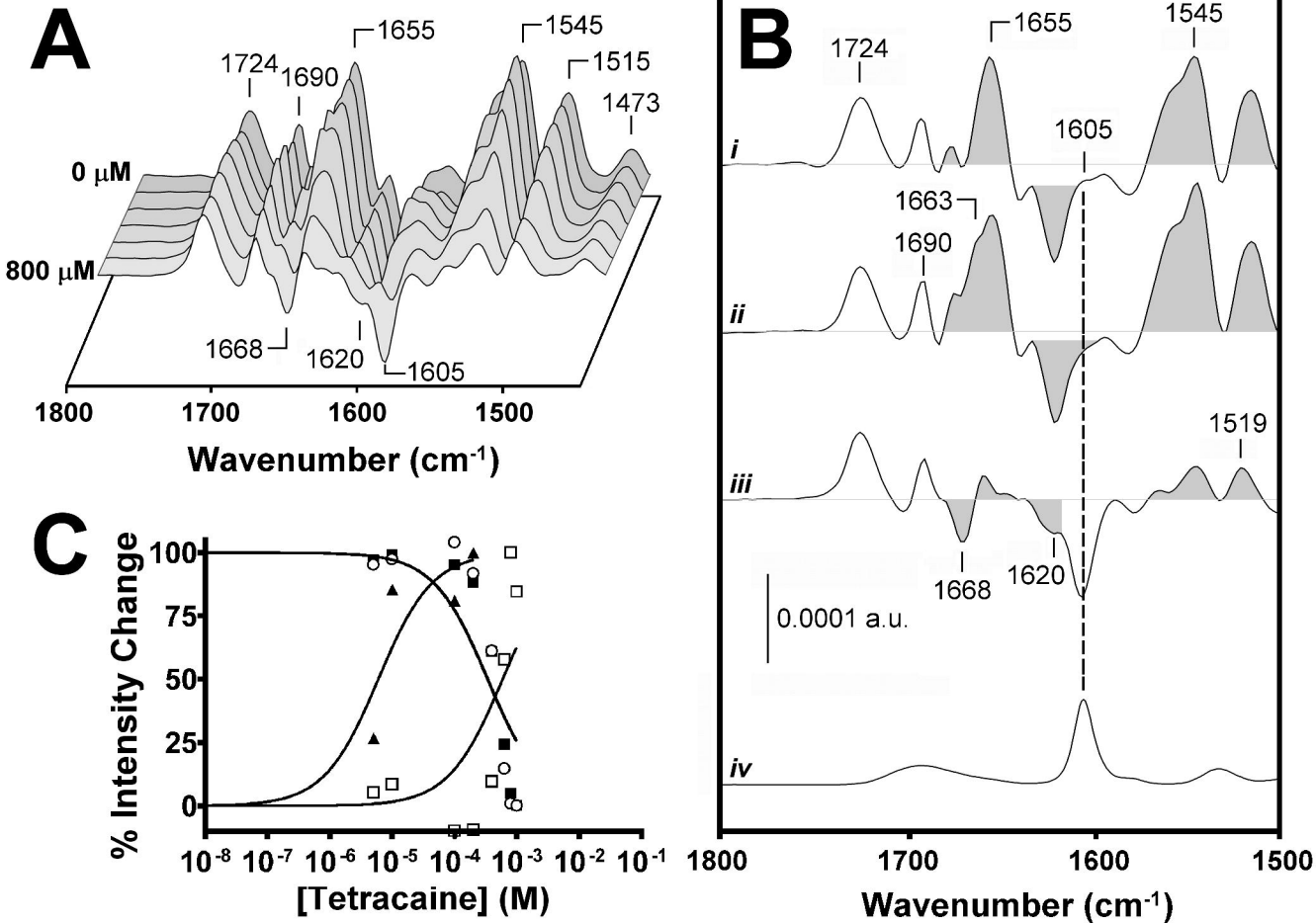
Figure 2

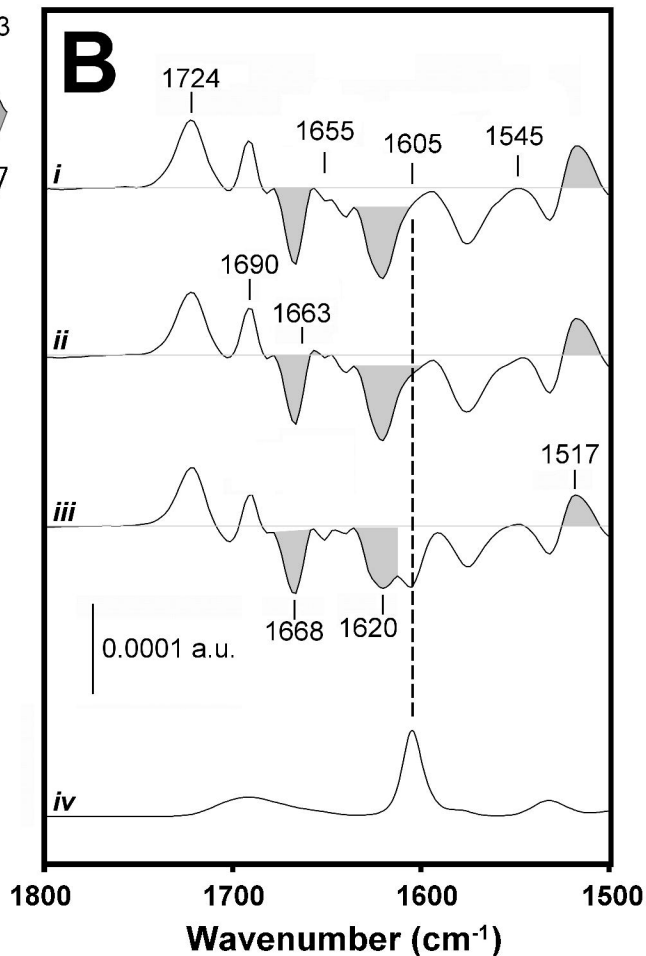
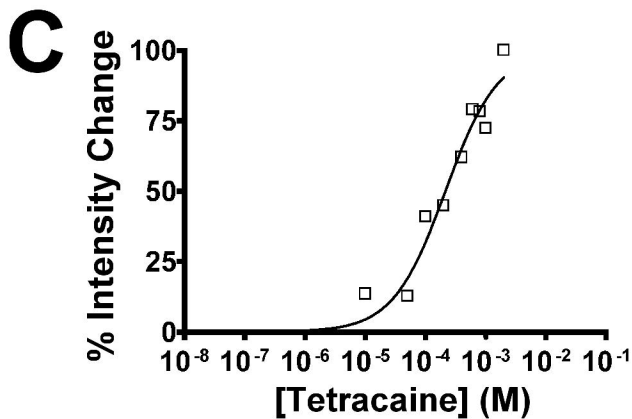
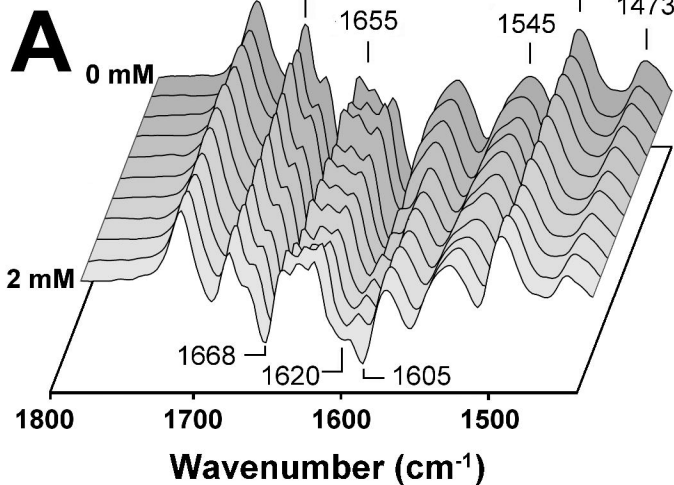
Figure 3

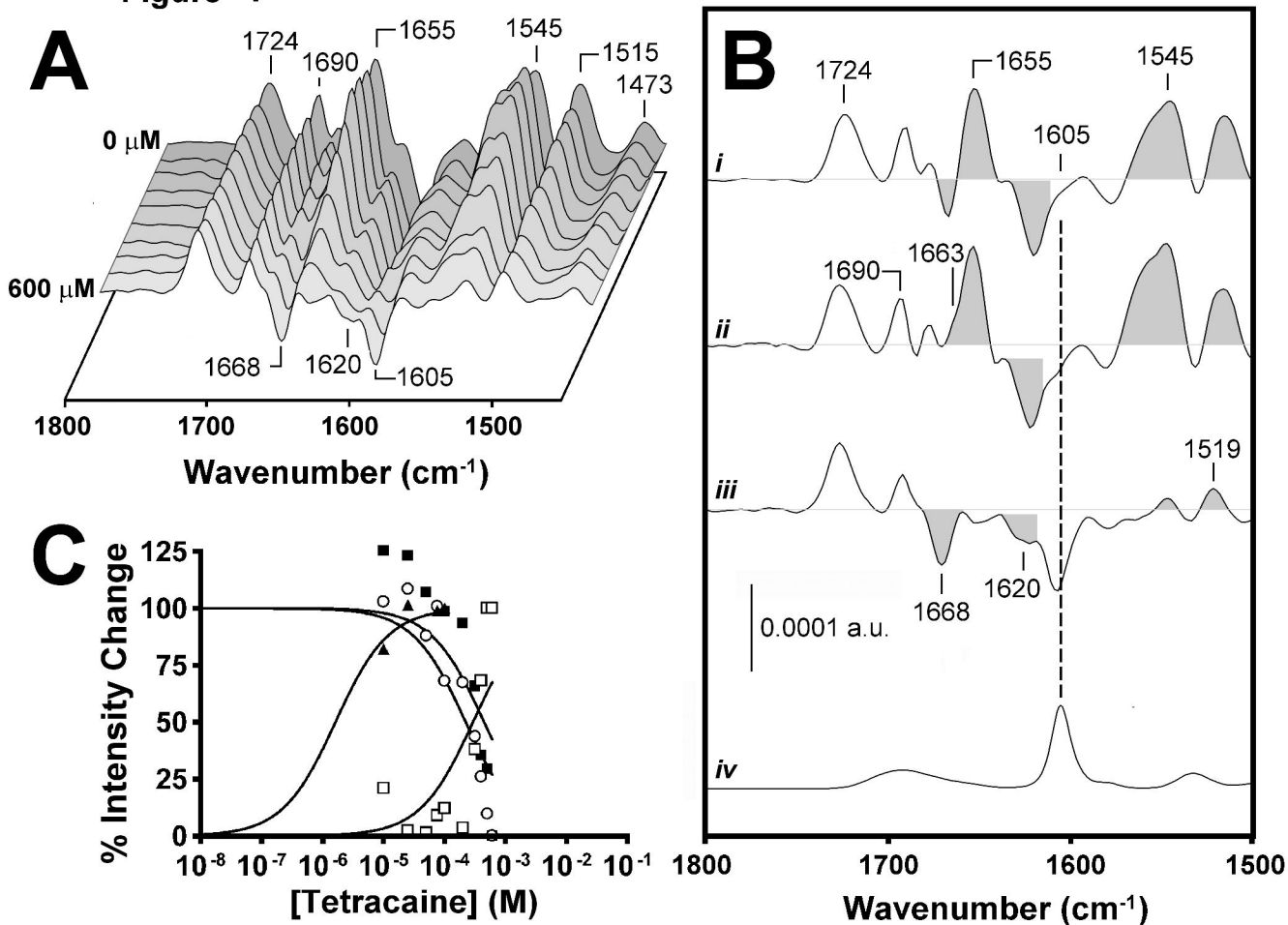
Figure 4

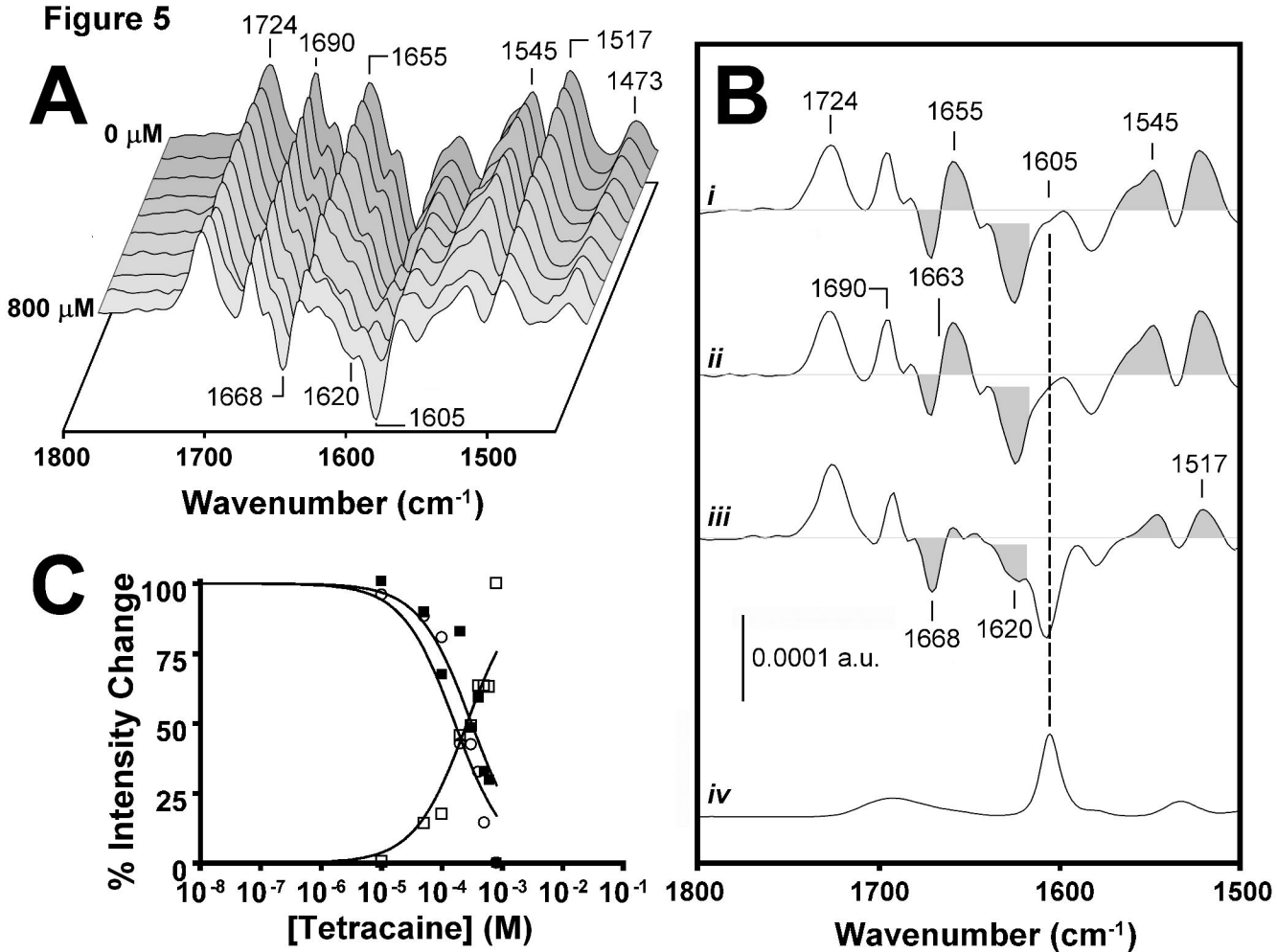
Figure 5

Figure 6

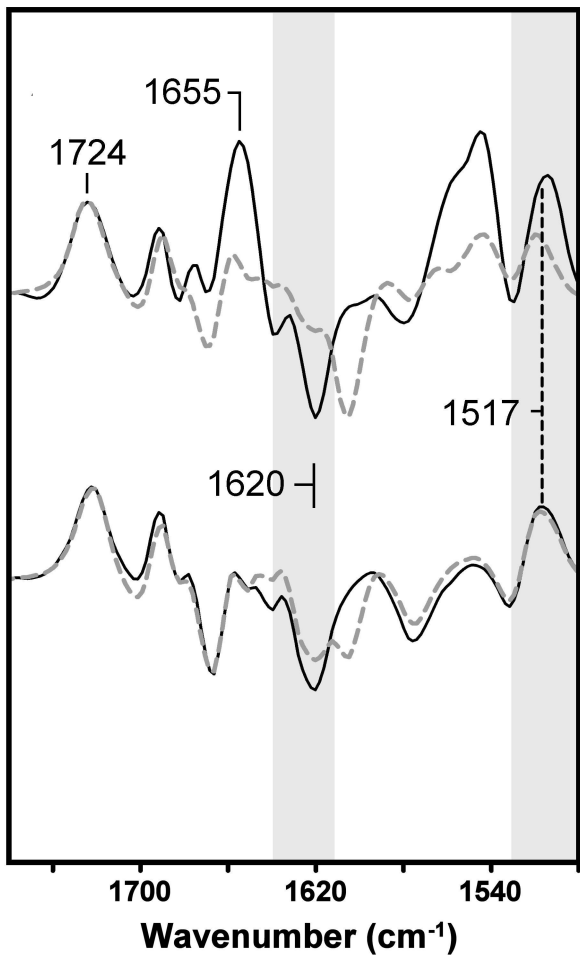


Figure 7

